The Mechanical Properties of Geopolymers as a Function of Their Shaping and Curing Parameters

Camille Zoude, Elodie Prud'Homme, Kévyn Johannes, Laurent Gremillard

ceramics

MDPI

Article

The Mechanical Properties of Geopolymers as a Function of Their Shaping and Curing Parameters

Camille Zoude [1,*], Elodie Prud'homme [1], Kévyn Johannes [2] and Laurent Gremillard [1]

[1] INSA Lyon, Université Claude Bernard Lyon 1, CNRS, MATEIS, UMR5510, 69621 Villeurbanne, France; elodie.prudhomme@insa-lyon.fr (E.P.); laurent.gremillard@insa-lyon.fr (L.G.)
[2] INSA Lyon, Université Claude Bernard Lyon 1, CNRS, CETHIL, UMR5008, 69621 Villeurbanne, France
* Correspondence: camille.zoude@insa-lyon.fr

Abstract: This study investigates the impact of curing conditions, porosity and shaping techniques on the mechanical properties of metakaolin-based geopolymers. Geopolymers offer versatility in shaping, including 3D printing, yet the influence of curing conditions after printing on mechanical properties remains unclear. This is assessed by measuring the bending properties of 3D-printed metakaolin-based geopolymer filaments cured under varied humidity and temperature conditions. The influences of porosity and of shaping technique are observed by comparing the compression properties of molded and 3D-printed samples of various porosity. Samples cured at low humidity exhibit unusually high mechanical properties, which decrease when moved from a dry to a humid environment. This behavior may be due to the presence of PEG within the composition and/or to residual stresses due to the too rapid evacuation of water. High humidity is therefore necessary to ensure optimal curing and stable properties. Increasing the curing temperature helps accelerate geopolymerization without significantly compromising mechanical properties. Direct ink writing offers design flexibility and suitable porosity, but the samples appear to exhibit different failure mechanisms than the molded samples. Additional studies are necessary to understand the interactions between PEG and the geopolymer as well as to better identify the fracture mechanisms within the different samples.

Keywords: direct ink writing; porosity; bending strength; compressive strength; molding

Citation: Zoude, C.; Prud'homme, E.; Johannes, K.; Gremillard, L. The Mechanical Properties of Geopolymers as a Function of Their Shaping and Curing Parameters. *Ceramics* **2024**, *7*, 873–892. https://doi.org/10.3390/ceramics7030057

Academic Editors: Maurice Gonon, Sandra Abdelouhab and Gisèle Laure Lecomte-Nana

Received: 3 April 2024
Revised: 31 May 2024
Accepted: 14 June 2024
Published: 25 June 2024

1. Introduction

Geopolymers are inorganic materials obtained generally by the alkaline activation of an aluminosilicate source at temperatures below 100 °C.

The geopolymer formation reaction, called geopolymerization, begins with the dissolution of the aluminosilicate source in the alkaline solution to form monomers. These monomers restructure to form oligomers which, beyond a critical concentration, polycondense, leading to the formation of a gel and the development of an amorphous, three-dimensional aluminosilicate network [1]. Metakaolin is a widely used aluminosilicate source for geopolymer manufacturing because it is a common industrial mineral that can be obtained in large quantities with consistent properties [2].

Generally, geopolymers are shaped by molding. During curing, molds are kept hermetically sealed to avoid the rapid evaporation of water which could lead to incomplete geopolymerization and poor mechanical characteristics. Perera et al. [3] observed that metakaolin-based geopolymers cured between 30% and 70% relative humidity in unsealed containers at 40 °C exhibited cracks, unlike those left sealed and cured between 22 and 60 °C. Samuel and Kriven [4] found in a recent study that curing the metakaolin-based geopolymer in low relative humidity from the time of molding resulted in a gradient in the extent of the reaction from the exposed surface to the bulk: the surface of geopolymers presented a mixture of geopolymer, alkaline silicate gel and undissolved metakaolin. Several authors have demonstrated the significant influence that curing temperature can

have on the mechanical properties of metakaolin-based geopolymers placed in sealed molds. Curing at elevated temperatures (up to 80 °C) accelerates the development of geopolymer strength [2,5,6].

Recently, 3D printing has emerged as a popular method for shaping geopolymers, offering significant flexibility in design. This shaping technique is applied mostly in the field of construction. Theoretically, it offers several advantages over traditional construction methods, such as shortened construction timelines, architectural design freedom, better safety at work and reduced labor, costs and waste [7]. However, this technique also enables the production of geopolymers with controlled porosity, suitable for diverse applications such as encapsulating radioactive waste, adsorbing hazardous molecules and synthetic dyes or heterogeneous catalysis [8–13]. These 3D-printed geopolymers are often printed under ambient temperature and humid conditions, and their size does not always allow for curing under controlled conditions. Furthermore, the resulting shapes often diverge substantially from traditional casts, particularly in the case of 3D printing through material extrusion, where filaments are assembled layer by layer, resulting in distinct mechanical properties. Nevertheless, there is no comprehensive study on the impact of environmental humidity and temperature on the mechanical properties of additively manufactured geopolymers.

This work is divided into two complementary studies. The first study investigates the effect of curing parameters (humidity and temperature) on the bending mechanical properties of metakaolin-based geopolymer filaments extruded using a 3D printer. These tests enable the rapid assessment of the mechanical properties of multiple filaments cured under varied conditions, rather than printing more intricate components.

The second part of this work compares the compression mechanical properties of geopolymer samples molded and 3D printed via extrusion and filament assembly (direct ink writing of lattices). The curing conditions for these samples remained constant to isolate the influence of the shaping technique and sample porosity on mechanical properties. The compositions of these samples were predetermined in a prior study focusing on characterizing the porosity of different metakaolin-based geopolymer compositions shaped by molding or 3D printing [14].

2. Materials and Methods

2.1. Raw Materials

The primary mix for the geopolymer includes metakaolin ARGICAL-M 1000, provided by Imerys, Paris, France (aluminosilicate source), a commercial sodium silicate solution (molar ratio: Si/Na = 1.1, density: 1.5 g.cm^{-3}, 60 wt.% water) and sodium hydroxide pellets (97% purity), both obtained from Fisher Scientific, Loughborough, UK, and used as alkaline activators. The geopolymers obtained are made of 43.7 wt% metakaolin, 51.8% sodium silicate and 4.5% sodium hydroxide.

Additives were added to this mixture to achieve specific characteristics [14]:

- Polyethylene glycol (PEG) with an average molecular weight of 1500 g·mol^{-1} (PROLABO, Paris, France) was used to induce a shear thinning behavior necessary for printing.
- To study the impact of porosity on the mechanical properties of geopolymers, metallic aluminum powder (Thermo Fisher, 99.5% purity, particle size less than 45 µm), referred to as Al, was introduced to generated dihydrogen and therefore porosity inside the paste, thanks to the following reaction:

$$2Al + 2NaOH + 2H_2O \rightarrow 2NaAlO_2 + 3H_2 \quad (1)$$

- Hexadecyltrimethylammonium bromide (CTAB, Sigma-Aldrich, St. Louis, MI, USA), a surfactant, was added to stabilize the gas bubbles.

2.2. Paste Preparation

The activation solution was first prepared by dissolving sodium hydroxide pellets and, depending on the composition, polyethylene glycol flakes, into sodium silicate solution. The mixture was stirred until all solids were fully dissolved and the solution returned to room temperature. Subsequently, it underwent homogenization using a planetary mixer (SpeedMixer, Synergy Devices Limited, High Wycombe, UK) for 30 s at 800 rpm.

Metakaolin, and CTAB when needed, was then gradually introduced and manually mixed for 30 s. The mixture was then placed for 1 min in the planetary mixer at 800 rpm.

For mixtures containing aluminum powder, this duration of mixing was reduced to 30 s because the mixture was subjected to a final mixing step, during which the aluminum powder was added. The paste containing the aluminum powder was mixed again in the planetary mixer for 30 s.

All the geopolymers in this study present the following molar ratios: SiO_2/Al_2O_3 = 3.73, Na_2O/Al_2O_3 = 0.95 and H_2O/Na_2O = 10.5.

2.3. Sample Preparation

The final mixture was poured into different containers depending on the tests to be performed:

- For compression tests, 16 × 16 × 20 mm^3 rectangular molds;
- To print lattices and filaments containing PEG for compression and three point bending tests, 5 mL syringes (Nordson EFD, USA);
- For three point bending tests of filaments without PEG (which cannot be printed), Teflon mold pierced with 2.5 mm diameter holes.

If the mixture did not contain aluminum powder, the containers were directly sealed to prevent any evaporation of water. If the mixture contained aluminum powder, the samples were left in the open air for 20 min to allow the foam to form. Excess foam was removed using a glass slide, and the containers were sealed.

All containers remained for one hour (from the addition of metakaolin) at room temperature.

After that time, the paste contained in the syringes was shaped by direct ink writing using a Robocasting printer (3D-Inks, Tulsa, OK, USA) equipped with tips of 840 µm inner diameter (Nordson EFD, USA). This step took place at room temperature (between 20 and 24 °C) and ambient humidity.

Two types of parts were printed: 17 mm long filaments (on a single layer) and porous lattices of 13.7 × 13.7 × 11.8 mm^3.

To print filaments, the needle was placed 1 mm above the printing substrate to avoid any compression of the filament on the support. Extrusion was completed in less than 10 min.

In the case of lattices, filaments were assembled layer by layer, with an interpenetration of 12% of the tip diameter between two layers to ensure the cohesion of the structure. A disorientation of 90° between successive layers and an 840 µm hollow space (1.68 mm center to center) between filaments of the same layer was imposed.

Lattices and filaments were deposited on a printing substrate made of a flat glass plate covered with a sheet of smooth polymer (copier polyester transparent film).

Once printing was completed, the samples (molded and printed) were subjected to the curing conditions described in the following part.

2.4. Curing of the Samples

In the case of lattices and molded geopolymer, the samples were subjected to the curing protocol described in Figure 1. The last step allows for the elimination of water potentially contained within the samples before the testing protocols.

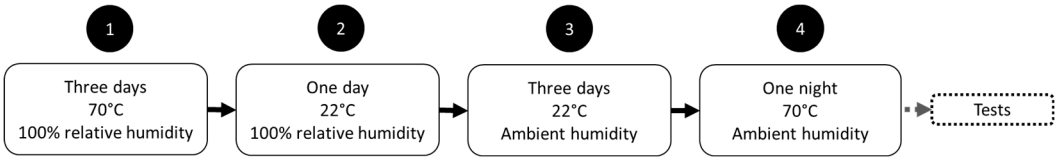

Figure 1. Curing protocol for molded geopolymers and lattice geopolymers.

In the case of 3D-printed filaments containing PEG, several curing conditions were tested. Filaments were subjected to six different curing conditions for periods up to 28 days. Three different temperatures were tested: 22 °C (room temperature), 50 °C and 70 °C. They were combined with two relative humidity (RH) conditions, 100% relative humidity and relative humidity less than 30%. At room temperature, curing took place in sealed boxes, one with the bottom covered with distilled water to reach 100% relative humidity and the other with silica gel at the bottom to achieve relative humidity below 30%. Curing at 50 °C and 70 °C took place in ovens. Samples were simply placed in the ovens in the case of curing at relative humidity below 30% (ambient humidity). For curing at 100% relative humidity, samples were placed in a carefully closed desiccator above a layer of distilled water.

Filaments without PEG, molded in Teflon molds, were subjected to only two different curing conditions: 70 °C at 100% relative humidity and 70 °C at less than 30% relative humidity. The mold was kept closed for two hours of curing to maintain the shape of the filaments. As a result, the low humidity curing condition was not completely observed during this time.

2.5. Samples Designation

The present article uses the same nomenclature as [14]. Geopolymers (G) are designated as follows:

$$\text{GPC } x\text{Al M/R/F}$$

where

- P signals the presence of 4.5 wt.% polyethylene glycol (with respect to the mass of metakaolin + sodium silicate + sodium hydroxide).
- C indicates the presence of 0.5 wt.% CTAB (with respect to the mass of metakaolin + sodium silicate + sodium hydroxide).
- xAl is the quantity of aluminum powder (0, 0.1, 0.2, 0.5 or 1 wt.% of metakaolin mass).
- M/R/F is the geopolymer shaping technique: molded (M), robocast as lattice (R) or robocast as filament (F).
- An absent letter (P or C) means that the composition does not contain the corresponding additive.

As an example, GPC 0.5Al R designates a geopolymer containing 4.5 wt.% PEG, 0.5 wt.% CTAB and 0.5 wt.% aluminum powder and shaped by robocasting (a lattice).

2.6. Samples Characterization

Porosity characterization is described in detail in a previous article [14]. This characterization was performed using three techniques: mercury intrusion porosimetry, helium pycnometry and X-ray tomography.

The mechanical bending properties of the filaments were tested via a three-point bending test on an Electroforce 3200 device (Bose, Eden Prairie, MN, USA) equipped with a 22 N force sensor at 0.3 mm.min^{-1} crosshead speed. At least 10 filaments were tested for each curing condition or composition.

Three-dimensional-printed filaments present a flat surface due to contact with the printing support (see Figure 2a). To minimize the impact of this flat surface on the test results, it was systematically placed on the compression side (in direct contact with the crosshead). Additionally, as the cross-sectional dimensions can vary significantly from

sample to sample, depending on the spread of the filament, the actual cross-sectional dimensions of each sample were measured using an optical microscope (Hirox Europe, Limonest, France) to calculate quadratic moment to each filament. The flexural strength to each filament was then calculated thanks to the following equation:

$$\sigma_f = \frac{F \times L}{4} \times \frac{x}{I_y} \quad (2)$$

where

- F: load applied to the center of the filament (N);
- L: distance between the two lower supports (set at 0.015 m);
- x: distance to neutral fiber in meters;
- I_y: quadratic moment in m^4.

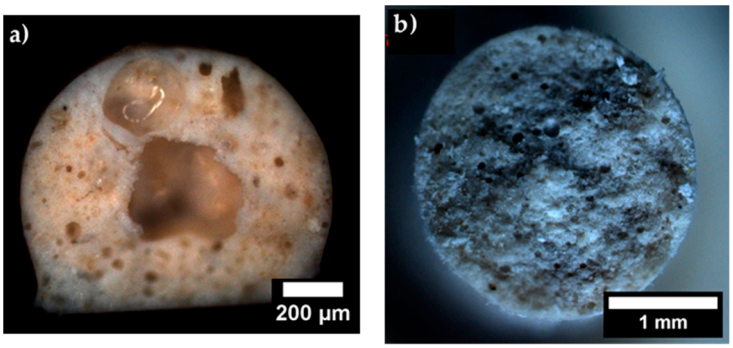

Figure 2. Optical microscope photographs of the fracture surfaces of (**a**) GPC 1Al F and (**b**) G 0Al F.

Filaments, which were molded (not containing PEG), are perfectly cylindrical (Figure 2b). Their section was compared to a disk, and their diameter was measured using a caliper. The equations can be therefore simplified as follows:

$$\sigma_f = \frac{8 \times F \times L}{\pi \times d^3} \quad (3)$$

where

- d: filament diameter (m).

Compressive mechanical properties of the lattices and molded geopolymers were tested using an Instron electro-mechanic universal testing machine (Instron 8500 +, Elancourt, France) equipped with a 25 kN (for sample G and GP) or 5 kN load cell (for other samples) crosshead speed of 0.3 mm · min^{-1}. Load/displacement curves were recorded and converted in stress/strain curves using the apparent section of each sample.

To highlight certain bonds and chemical groups, FTIR spectra were obtained using a Thermo Fisher Scientific (Waltham, MA, USA) IS50 infrared spectrometer via the attenuated total reflection (ATR) mode. The IR spectra were gathered between 500 and 4000 cm^{-1} with a resolution of 0.482 cm^{-1} on 32 scans. The atmospheric CO_2 contribution was replaced by a straight line between 2400 and 1900 cm^{-1}, and the spectra were corrected using a baseline. They were normalized on the peak of the Si-O-Na bond.

The filament fracture surfaces were observed using a SEM Vega 3 scanning electron microscope (Tescan, Brno, Czech Republic) equipped with a tungsten filament. Observations were carried out in secondary electron (SE) mode at 10 kV, with a working distance of 10 mm and a beam intensity of 8.

X-ray microtomography was performed on extruded filaments with a diameter of 840 µm using an RX Solutions (Chavanod, France) EasyTom Nano tomograph equipped with a Hamamatsu tube, at a resolution of 0.7 µm. Images were extracted using Fiji software.

3. Results

Bending tests, infrared spectroscopy and SEM observations were performed on dense filaments to evaluate the impact of curing conditions on mechanical properties and the microstructure. Compression tests were implemented on scaffolds and molded samples with one single curing condition to evaluate the impact of the shaping technique and porosity on compression properties.

3.1. Three Point Bending Tests on Dense Filaments

GP 0Al F were printed by direct ink writing, cured under different conditions and then subjected to the test. Six storage conditions were tested: three different temperatures (room temperature, 50 °C, 70 °C) combined with two humidity conditions (relative humidity less than 30% and relative humidity 100%). The evolution of mechanical properties was recorded at 24 h, 3 days, 14 days and 28 days. Figure 3 presents the evolution of the flexural strength according to the different conditions.

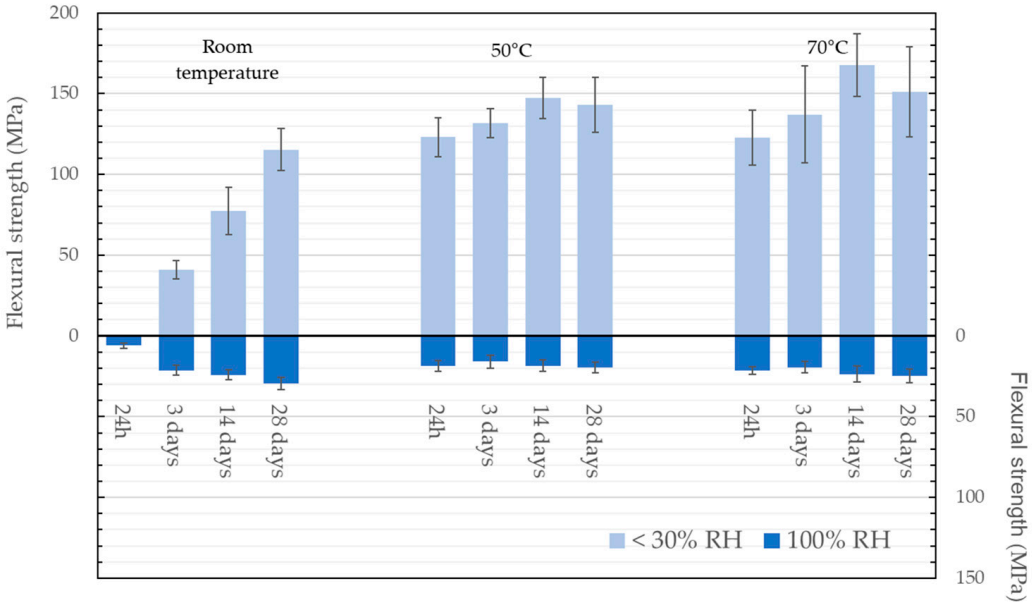

Figure 3. The flexural strength evolution of GP 0Al F as a function of time, relative humidity and the temperature of the environment.

Every filament exhibits brittle fracture (Figure 4), except filaments subjected to a relative humidity lower than 30% at room temperature and tested after 24 h and 3 days of curing. Indeed, under these conditions, after 24 h of curing, the filaments do not break but instead deform plastically until they are no longer in contact with the test supports (Figure 5). No cracks are observed on the surface. The filaments break after 3 days of storage but still show strong plastic deformation. However, this deformation is no longer visible after 14 days of curing (Figure 4a).

A significant difference is observed between the flexural strength of filaments stored at low relative humidity and those stored at high relative humidity, regardless of the temperature (Figure 3). Filaments cured at low humidity have an average flexural strength 5.5 times higher than filaments stored at high humidity after 28 days.

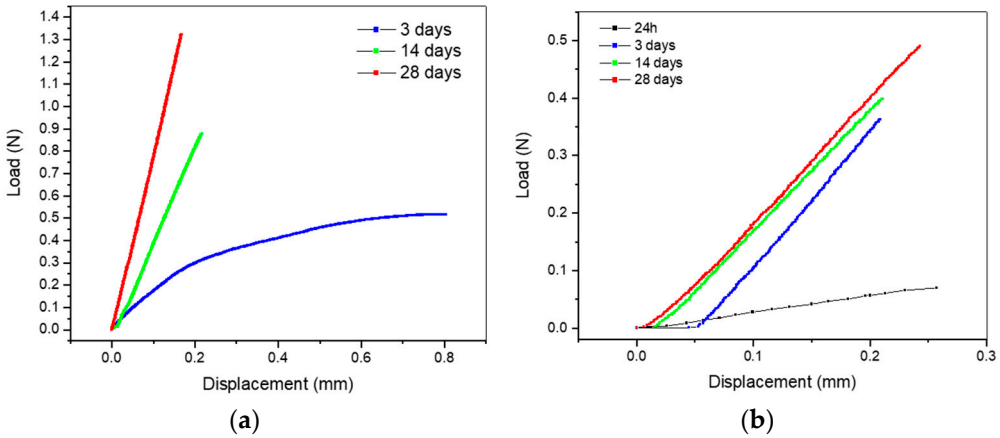

Figure 4. Typical load/displacement curves of GP 0Al F cured at room temperature and (**a**) relative humidity below 30% and (**b**) 100% relative humidity.

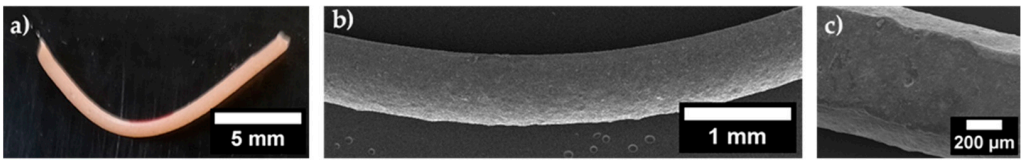

Figure 5. Digital (**a**) and electronic (**b**,**c**) micrographs of GP 0Al F following three-point bending test after 24 h of curing at room temperature below 30% relative humidity.

Samples stored at high humidity and at a temperature of 50 °C or 70 °C reach a flexural strength very close to the flexural strength obtained after 28 days within 24 h (about 20 MPa). It takes between 24 h and 3 days of curing for samples stored at room temperature to approach the 28-day flexural strength. It appears that the higher the temperature, the higher the average flexural strength. The same trend is noted in the literature on compression tests [15]. However, the results presented here are subject to high uncertainty, and these tests should be conducted on a larger sample population to confirm the trend.

Samples subjected to low humidity during curing exhibit a slower attainment of their maximum mechanical properties, especially at room temperature, where the flexural strength consistently increases throughout the 28-day testing period. The increase in temperature accelerates the increase in the strength since after 24 h at 50 °C or 70 °C, the flexural strength is already very close to the flexural strength reached at room temperature after 28 days (36 GPa). They continue to increase, reaching in both cases approximately 42 GPa after 28 days.

To assess the stability of these mechanical properties against humidity variations, GP 0Al filaments conditioned at a specific humidity and temperature for 28 days undergo two additional days of storage in inverted humidity conditions at room temperature. They are then subjected to the three-point bending test. Figure 6 presents the results before and after the change of condition.

The flexural strength of samples stored for 28 days at high humidity is not modified after 48 h at low humidity.

However, after 48 h at high humidity, the very high flexural strength of samples cured for 28 days at low humidity decreases. Filaments initially stored at room temperature display a flexural strength even lower than those stored at high humidity for 28 days. The final flexural strength of samples initially stored at 50 °C and 70 °C is slightly higher on average than that of samples stored at high humidity for 28 days at the same temperatures.

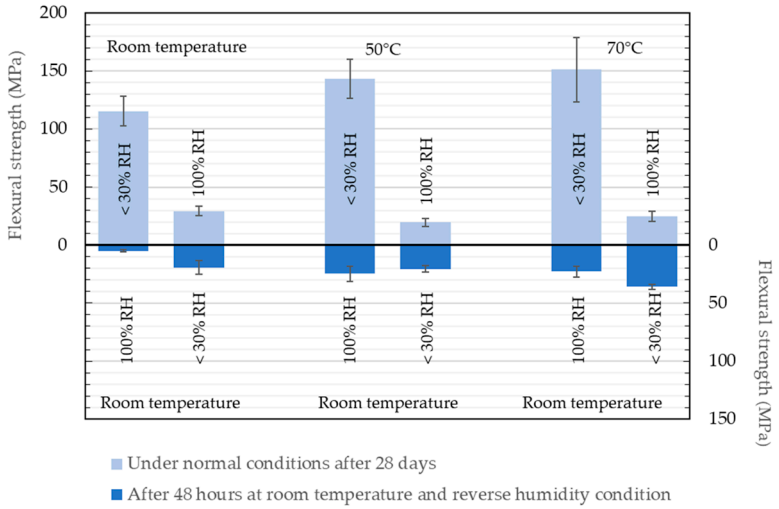

Figure 6. Flexural strength evolution of GP 0Al F before and after modification of curing conditions.

To determine if the addition of PEG impacts the mechanical properties of the filaments, a three-point bending test was performed on PEG-free filaments (G 0Al F). As the paste is not suitable for filament extrusion by direct ink writing, the filaments were molded into Teflon molds. Given the delicate nature of implementing this method and the very limited number of filaments obtained, only two conservation conditions were tested: 70 °C at 100% relative humidity and 70 °C at less than 30% relative humidity. Measurements were carried out at 14 days and are summarized in Table 1.

Table 1. Flexural strength of G 0Al F under different humidity conditions after 14 days at 70 °C.

	Flexural Strength (MPa)	
	<σ_f>	**SD**
<30% RH	29.7	6.7
100% RH	20.1	8.7

The significant difference in flexural strength observed as a function of humidity is not evident. The flexural strength of PEG-free filaments at low humidity is slightly higher than that at high humidity, but considering measurement uncertainties, they are quite similar. These values are also very close to those of the GP 0Al filaments stored at 100% relative humidity at the same temperature and after 14 days.

Thus, the high mechanical properties observed at low humidity seem to be influenced by the presence of polyethylene glycol. A comprehensive discussion of the role of PEG, considering additional results, will be discussed in Part 4.

However, it is already apparent that, in the case of geopolymer compositions containing polyethylene glycol, it is more prudent to print and store the samples under high relative humidity to ensure the stability of mechanical properties.

3.2. Infrared Spectroscopy of Dense Filaments

After being stored under the different conditions described above, GP 0Al F were ground and analyzed using infrared spectroscopy (ATR mode).

3.2.1. Filaments Stored 28 Days at Low Humidity

PEG is constantly detected in filaments that have been stored 28 days at low humidity regardless of the conservation temperature (Figure 7).

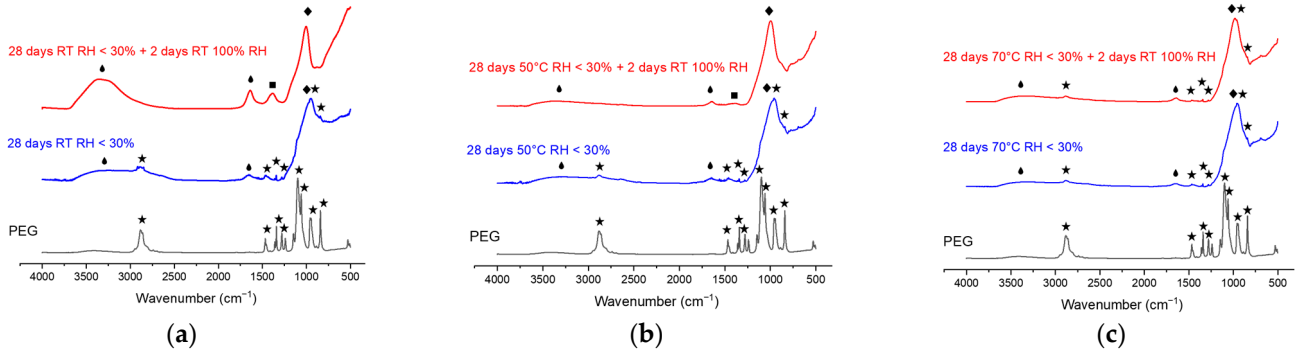

Figure 7. Normalized infrared spectra of crushed filaments GP 0Al F and PEG 1500. GP 0Al filaments were cured 28 days at relative humidity below 30% and (**a**) room temperature or (**b**) 50 °C or (**c**) 70 °C before being placed 2 days at room temperature and high relative humidity. ♦: Vibrational bands of water binding [16,17]; ★ vibrational bands of PEG binding [18]; ■ vibrational bands of carbonate binding group [17]; ◆ vibrations of the characteristic binding of the geopolymer network [19].

After 28 days, when the humidity conditions are reversed for two days, PEG is no longer detected, except in the case where the filaments have been stored 28 days at 70 °C. A peak associated with the presence of carbonate is detected during this humidity condition inversion for filaments stored at room temperature and 50 °C. It is particularly pronounced for filaments stored at room temperature.

3.2.2. Filaments Stored 28 Days at High Humidity

PEG is not detected in filaments that have been stored 28 days at high humidity (Figure 8). All filaments present a significant peak associated with carbonates. When reversing the humidity conditions, PEG was still not detected in filaments that have been stored at room temperature and 50 °C. On the other hand, it is detected in filaments that have been stored at 70 °C. The carbonate peak is consistently present, whether before or after reversing humidity conditions.

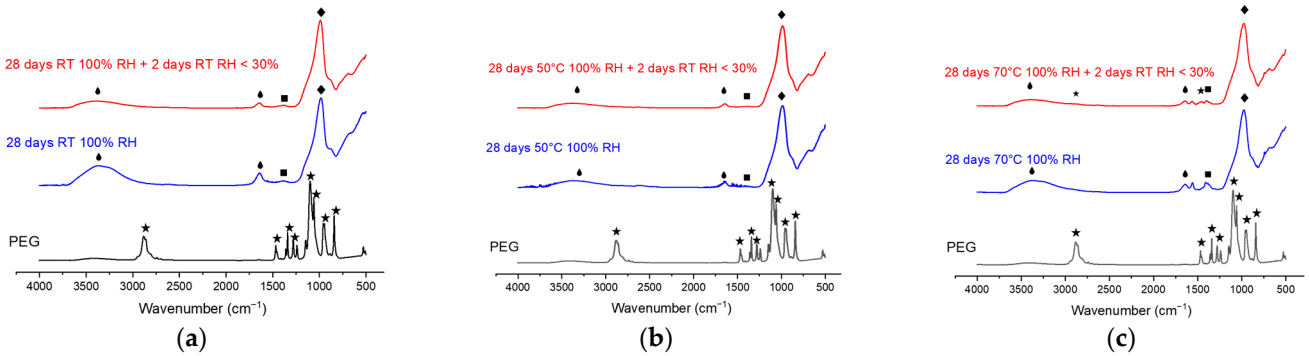

Figure 8. Normalized infrared spectra of crushed filaments GP 0Al F and PEG 1500. GP 0Al filaments were cured 28 days at high relative humidity and (**a**) room temperature or (**b**) 50 °C or (**c**) 70 °C before being placed 2 days at room temperature and relative humidity below 30%. ♦: Vibrational bands of water binding [16,17]; ★ vibrational bands of PEG binding [18]; ■ vibrational bands of carbonate binding group [17]; ◆ vibrations of the characteristic binding of the geopolymer network [19].

3.3. Fracture Surface of Dense Filaments

The morphology of the fracture surfaces of filaments cured at room temperature varies depending on the environmental humidity (Figure 9). Filaments stored in high humidity conditions exhibit a more spread-out structure with a substantial flat area, while those cured under low humidity are rounder with a smaller flat region, indicating a better preservation

of their original shape. As the filaments were extruded on the same day under consistent conditions, this phenomenon is likely to occur during the curing process.

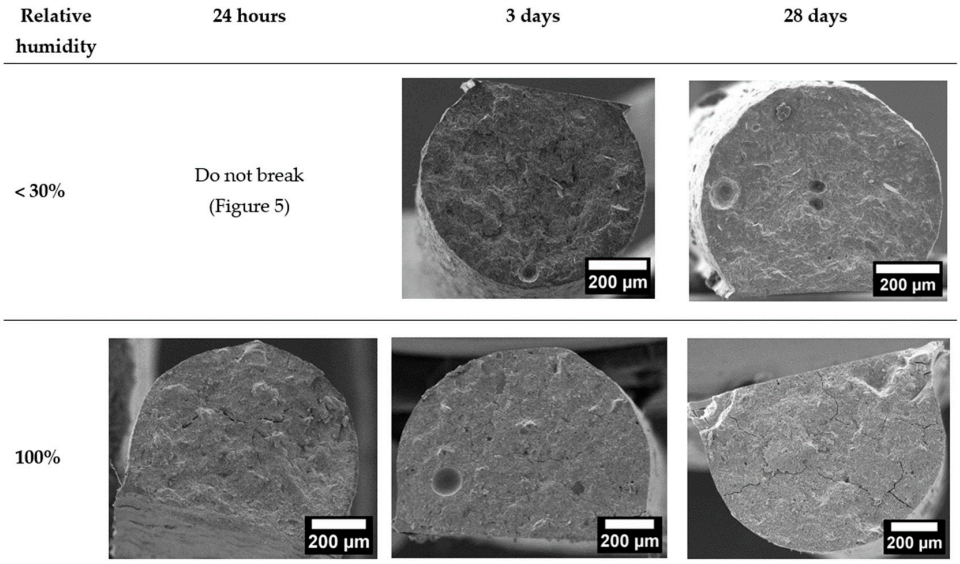

Figure 9. Fracture surface of GP 0Al cured at room temperature for 24 h, 3 days and 28 days under high and low relative humidity.

At high relative humidity, increasing the curing temperature appears to limit the spreading of the filaments (Figure 10).

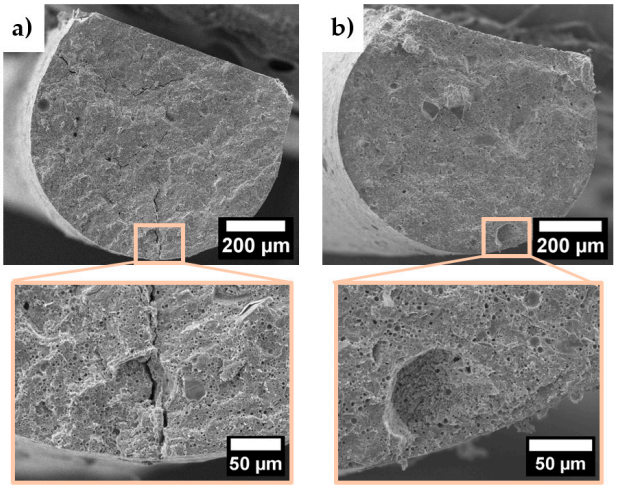

Figure 10. SEM micrographs of fracture surfaces of GP 0Al F after 24 h under 100% RH at (**a**) 50 °C and (**b**) 70 °C.

In addition, filaments stored at room temperature have different microstructures depending on the humidity of the environment.

The fracture surface of filaments stored at high humidity for 24 h exhibits large cracks and a microstructure with visible pores within a homogeneous mass (Figure 11a). After three days of curing, these pores become numerous and take on a well-defined spherical shape, similar to the microstructure observed after 28 days of curing (Figure 11b,c). Each time, more or less significant cracks are observed on the fracture surface. Increasing the curing temperature (50 °C and 70 °C) while maintaining high relative humidity results in a microstructure like that obtained after three days at room temperature and high humidity in only 24 h (Figure 10).

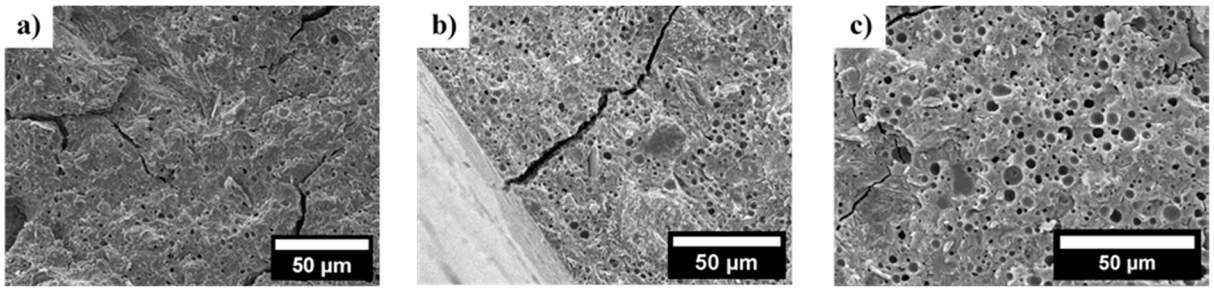

Figure 11. SEM micrographs of fracture surface of GP 0Al filaments cured at room temperature under 100% RH after (**a**) 24 h, (**b**) 3 days and (**c**) 28 days.

As mentioned previously, filaments cured at low humidity for 24 h are strongly deformed by the three-point bending test. Their surface shows no cracks (Figure 12). After three days of curing, the fracture surfaces exhibit irregularities, visually indicating the plasticity observed in the fracture curves (Figure 12a). Unlike samples stored at high humidity, only fine cracks are visible. Pores are also visible, but the geopolymer matrix seems less homogeneous. After 28 days of curing, the fracture surfaces are more clearly defined but seem to have a double microstructure. The interior of the filaments presents a microstructure similar to that observed after 24 h of curing in the case of filaments cured under high humidity (Figure 12b). However, the exterior of the filament has a very dense microstructure, with no visible porous network (Figure 12c).

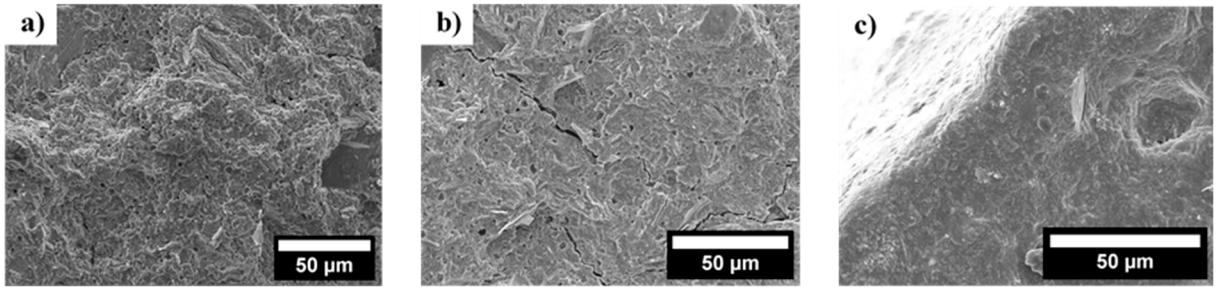

Figure 12. SEM micrographs of fracture surface of GP 0Al F cured at room temperature under low relative humidity after (**a**) 3 days, (**b**) 28 days (filament core) and (**c**) 28 days (filament periphery).

3.4. Compressive Stress of Molded Geopolymers and Lattices

3.4.1. Molded Geopolymers

Table 2 gathers the main properties of the geopolymer compositions studied in the previous work. Figure 13 shows one of their typical stress/strain curves.

It is evident that the compressive strength decreases with increasing porosity. All curves exhibit brittle behavior, with a linear elastic domain at low stresses followed by a more or less significant plateau typical of fragile foams [20]. The extent of the linear elastic phase, representing undamaged material, diminishes as porosity increases. The plateau following the linear phase is attributed to the collapse of the solid phase inside the material by the crushing of the walls between the pores. In GPC compositions (Figure 13b), higher quantities of aluminum powder led to the initiation of material damage at progressively lower stresses, but there is a notable increase in the allowed deformation before reaching fracture.

Table 2. Envelope density, total porosity and maximum compressive stress of molded geopolymers.

Designation	Envelope Density ($g.cm^{-3}$) ± SD	Total Porosity (vol.%)	Compressive Strength (MPa) ± SD
G 0Al M	1.43 ± 0.01	34.2 ± 3.1	50.8 ± 5.2
GP 0Al M	1.40 ± 0.01	36.7 ± 1.6	41.6 ± 9.9
GPC 0.1Al M	0.90 ± 0.06	58.3 ± 3.4	5.0 ± 0.4
GPC 0.2Al M	0.74 ± 0.03	66.0 ± 2.3	3.4 ± 0.8
GPC 0.5Al M	0.65 ± 0.07	70.1 ± 3.1	2.4 ± 0.8
GPC 1Al M	0.61 ± 0.02	71.6 ± 1.7	2.1 ± 0.4
GP 0.5Al M	0.43 ± 0.03	79.7 ± 1.7	1.3 ± 0.3
GC 0.5Al M	0.28 ± 0.02	87.0 ± 1.2	0.21 ± 0.05

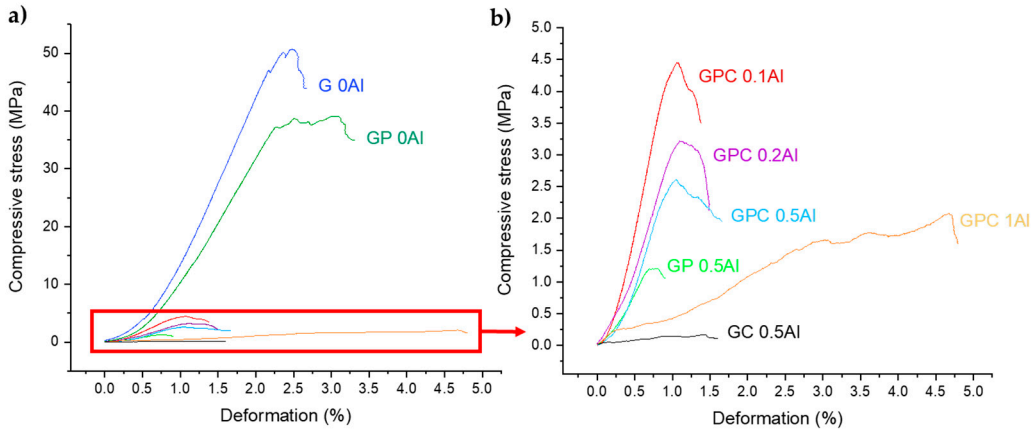

Figure 13. Stress/strain curves of all molded geopolymers (**a**) and composition manufactured with aluminum powder ((**b**): detail of (**a**)).

Figure 14 shows the evolution of the compressive strength as a function of the envelope density of the samples. A power law with a good correlation coefficient was chosen to represent this evolution. However, it tends to underestimate compressive strengths at lower envelope densities. Despite this limitation, this relationship provides an estimate of the expected compressive strength for molded geopolymers with similar composition.

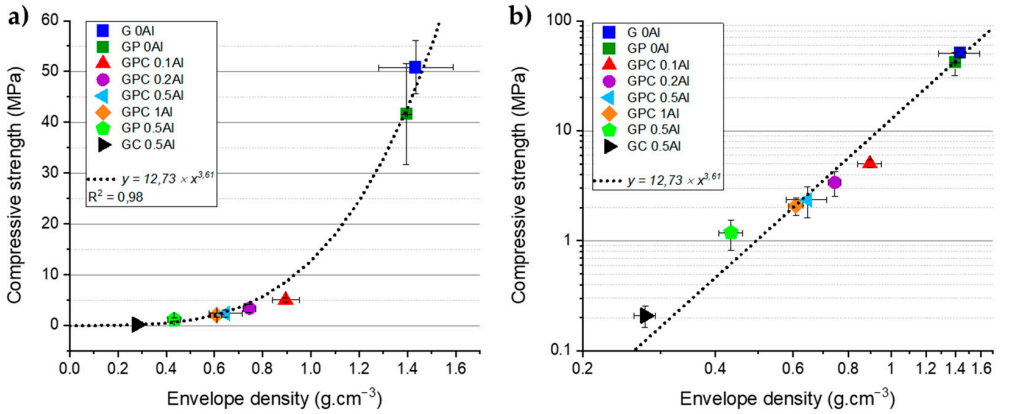

Figure 14. The evolution of the compressive strength as a function of the envelope density of the molded geopolymer samples in (**a**) linear and (**b**) logarithmic scale. Error bars represent standard deviations.

3.4.2. Three-dimensional-Printed Geopolymer Lattices

The main properties of the geopolymer lattices obtained by direct ink writing are summarized in Table 3. G 0Al R have greater porosity—and therefore lower compressive strength—compared to G 0Al M, thanks to the spacing between the filaments. The lattices made with 0.1, 0.2, 0.5 and 1% aluminum powder have similar total porosities (for more information, see [14]) and therefore similar compressive strengths.

Table 3. Envelope density, total porosity and maximum compressive stress of lattices.

Designation	Envelope Density ($g.cm^{-3}$) ± SD	Total Porosity (vol.%)	Compressive Strength (MPa) ± SD
GP 0Al R	1.08 ± 0.04	51.1 ± 2.7	18.3 ± 5.3
GPC 0.1Al R	0.83 ± 0.04	61.6 ± 2.4	2.7 ± 0.5
GPC 0.2Al R	0.70 ± 0.03	67.9 ± 2.3	3.3 ± 0.3
GPC 0.5Al R	0.75 ± 0.05	65.6 ± 3.3	3.2 ± 0.6
GPC 1Al R	0.74 ± 0.04	65.5 ± 2.8	3.0 ± 0.6

The stress/strain curves do not always present a linear elastic domain, likely due to local defects and the difficulty of obtaining perfectly parallel surfaces on these samples (Figure 15). The irregular decreases in stress could also be due to the progressive collapse of the layers by the fracture of the filaments, possibly at the junctions of the filaments, or by the propagation of cracks already present within the material.

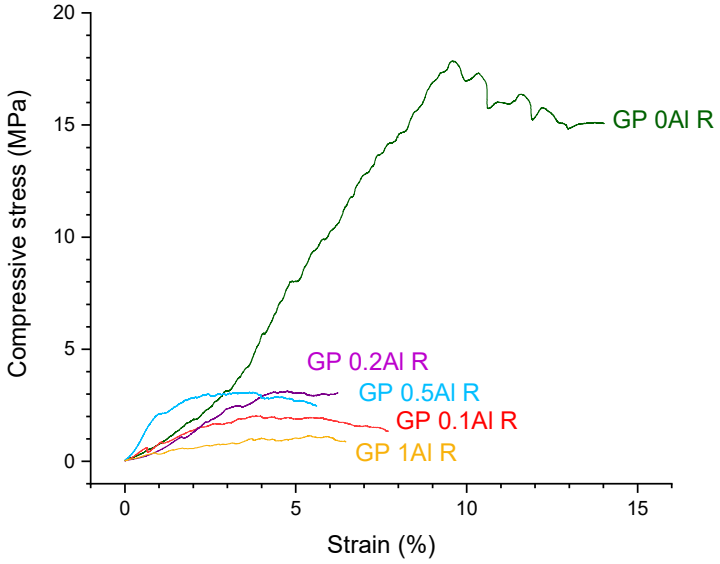

Figure 15. Stress/strain curves of geopolymer lattices.

The addition of the points corresponding to lattices on the evolution of the compressive strength as a function of the envelope density leads to a lower correlation coefficient (drop from 0.98 to 0.70, Figure 16). However, the points respect the general trend.

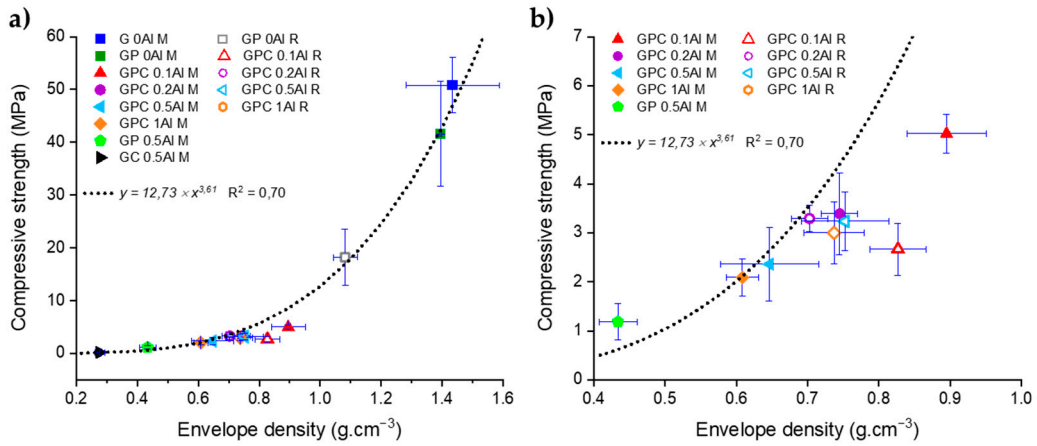

Figure 16. (**a**) The evolution of the compressive strength as a function of the envelope density of different geopolymer compositions shaped by molding and direct ink writing; (**b**) zoom of 16 (**a**). Error bars represent standard deviations.

4. Discussion

4.1. Influence of PEG and Curing Parameters on Filament Bending Stress

4.1.1. Impact of Storage at High Relative Humidity on the Properties of Geopolymers

At high relative humidity, Baird et al. [21] demonstrated that PEG 1450 absorbs atmospheric humidity through the phenomenon of deliquescence, transitioning from a solid to a solution by sorbing significant amounts of atmospheric moisture. Although this phenomenon depends on the molar mass of PEG and temperature, the study shows that the deliquescence of PEG 1450 at 25 °C begins at 66% relative humidity and at 49% relative humidity at 40 °C. Although our work involves a slightly different PEG (PEG 1500) and different temperatures (room temperature, 50 °C and 70 °C), this study's findings suggest that under our conditions, at 100% relative humidity, the polyethylene glycol in geopolymers is likely to undergo deliquescence. Part of PEG is probably in the liquid state, especially since the temperatures 50 °C and 70 °C are higher than the melting temperature of PEG 1500 (45 °C). This high relative humidity would allow for the conservation of a large quantity of water within the capillary network.

This presence of water explains the systematic detection of sodium carbonates in infrared spectroscopy after 28 days of storage at high humidity (Figure 8). Carbonate formation indeed requires water to dissolve the CO_2 present in the air [22]. This observation suggests that sodium is found in excess in the geopolymer network and is free to react to form carbonates. Thus, PEG is immersed in an extremely basic environment which could, over time, degrade it and explain why it is not detected in infrared spectroscopy after 28 days. But this could also be explained by the fact that the bonds constituting PEG are probably looser since it is in the liquid state, and its presence could be masked by the spectrum of water.

The liquid state of PEG at high humidity explains the greater spreading of the filaments cured in these conditions (Figure 9). The filament spreading diminishes progressively with rising temperatures (Figure 10), likely due to the accelerated geopolymerization process. Indeed, it takes between 24 h and 3 days for filaments stored at room temperature to reach mechanical properties close to the final properties (Figure 3). For storage of filaments at 50 and 70 °C, this time is reduced to less than 24 h. Increasing the curing temperature accelerates the geopolymerization at high humidity.

The presence of PEG does not affect the mechanical properties in the bending of geopolymer filaments cured at high humidity (Figure 3 and Table 1). Filaments with PEG present mechanical properties equivalent to compositions without PEG and close to the values reported in the literature, with a flexural strength between 10 and 20 MPa [2,23].

But the introduction of PEG has an impact on the mechanical properties in the compression of molded samples cured under high relative humidity. The compressive strength

decreases on average from 50.1 to 41.6 MPa after the addition of PEG (Table 2). This difference is more likely due to a difference in density as the molded samples containing PEG are more porous than the molded samples without PEG. Given the higher viscosity of pastes containing PEG [14], they are more prone to trapping air bubbles, potentially leading to sample failure. Despite this difference in mechanical properties in compression, the orders of magnitude obtained for these mechanical properties are consistent with those found in the literature (compressive strength around 50 MPa) [24].

4.1.2. Impact of Low Relative Humidity Storage on Geopolymer Properties

After curing at low relative humidity, the filaments exhibit unusually high mechanical properties, regardless of temperature and curing duration (Figure 3). However, filaments without PEG maintain normal mechanical properties regardless of humidity conditions (Table 1).

The first hypothesis to explain this phenomenon would be that PEG, which does not undergo deliquescence at low humidity, might act as a mechanical binder by solidifying and forming a continuous 3D network within the geopolymer. Its solid form is always detected in infrared spectroscopy after grinding filaments cured under these conditions (Figure 7). Despite curing temperatures of 50 °C and 70 °C exceeding PEG's melting point, there is a possibility that PEG rapidly solidifies within the structure upon returning to room temperature for the tests.

An alternative hypothesis emerges based on recent findings by Samuel and Kriven [4]. They conducted microhardness measurements on geopolymer bars cured at 20 °C and 40% RH, revealing notably high surface microhardness over an approximate thickness of 2 mm. The authors attribute this phenomenon to potential residual stresses near the surface induced by capillary stresses from rapid water evacuation and/or density variations within the material due to these stresses. Given the small size of the filaments in this study (840 µm in diameter), it is plausible that these residual stresses contribute to the observed significant mechanical properties, especially considering the filaments exhibit a density gradient after 28 days of curing (Figure 12b,c). The rapid evacuation of water and the stresses generated may be sufficient to prevent filament spreading. The fact that the PEG-free sample did not exhibit high properties at low humidity (Table 1) could be since the mold was opened two hours after molding the filaments, to allow them to retain their shape. These two hours in endogenous conditions were perhaps enough to modify the constraints within the filament. In this scenario, PEG does not act as a mechanical binder, although present in the structure (because detected in infrared).

Finally, it is possible that these unusually high mechanical properties at low humidity can be explained by a combination of these two hypotheses, with PEG acting as a mechanical binder, residual stresses and density variation. Additional tests must be carried out to achieve a more comprehensive understanding of the phenomena.

These hypotheses are consistent with the fact that filaments cured at low humidity and room temperature for up to 3 days deform plastically, while filaments cured at high humidity do not (Figures 4 and 5). Samuel and Kriven [4] observe a similar behavior on geopolymer bars without PEG. This behavior becomes more pronounced with the decrease in the amount of water introduced into geopolymer pastes. The curing process at low humidity may prevent the retention of a sufficient water quantity within the capillary network. The hygroscopic nature of polyethylene glycol could contribute to this effect, resulting in insufficient water availability for proper species dissolution and network formation. Additionally, unlike filaments cured at high humidity, there is no discernible carbonation peak (Figure 7), indicating insufficient water for carbonate formation (where sodium is necessarily present). The geopolymerization phenomenon, already slower at room temperature than at 50 and 70 °C, would therefore be further slowed down. The material would be composed of partially dried alkaline silicate, partially solid polyethylene glycol and geopolymer/metakaolin particles. These components would form a deformable gel, which can be further reinforced by the presence of PEG, and which would constitute the

mechanical skeleton of the geopolymer during the first 24 h, while the geopolymerization takes place slowly until influencing the fracture behavior. However, this geopolymerization at room temperature and low humidity is clearly incomplete. When the storage conditions are reversed, the flexural strength of the filaments collapses below the anticipated level, equivalent to the flexural strength of filaments stored at high humidity, which formed their own geopolymer network without being influenced by rapid water drainage (Figure 6). In addition, a very significant carbonation peak is detected in infrared spectroscopy (Figure 7a). This is probably due to the rehydration of the sodium-containing species which did not have time to react to form the geopolymer network before curing. Consequently, sodium returns to solution due to high ambient humidity and reacts to form carbonates. Moreover, the microstructure of the filament is very dense after 3 days of storage, and only the core of the filament shows the signs of a porous network characteristic of a geopolymer after 28 days of curing (Figures 9 and 12).

Samuel and Kriven [4] also observed incomplete geopolymerization on the surface of their samples without PEG stored at 20 °C and 40% RH.

Filaments cured at low humidity at 50 °C and 70 °C do not exhibit plasticity during the first curing days (Figure 4a). But these samples also exhibit unusually high mechanical properties. When humidity conditions are reversed, these properties collapse to levels comparable to filaments cured at high humidity (Figure 6). Following this reversal, the infrared band of PEG is nearly absent, and the carbonation signal is notably reduced compared to filaments cured at low humidity and room temperature. These observations suggest that the geopolymer network was well formed and that the transition to high humidity caused either the deliquescence of the PEG, rendering it ineffective as a binder (resulting in a mechanical structure purely made of geopolymer), or the relaxation of the constraints within the structure or both.

Several hypotheses can be considered and combined to explain this more complete formation of the geopolymer network at 50 and 70 °C at low humidity. First, the temperature increase accelerates geopolymerization reactions sufficiently to occur, while there is still enough water in the medium. Then, the melting temperature of PEG might be exceeded in the case of curing at 50 °C and 70 °C. The PEG being in a liquid form, its hygroscopic nature might be limited, and more water could be found within the structure in the early stages. Despite efforts to minimize the time between exiting the oven and conducting the bending test, the rapid cooling of the small filaments (840 µm in diameter) may result in the quick return of PEG to a solid state, resuming its role as a binder during the test.

These observations indicate that it is not the presence of PEG that limits geopolymerization and confers plasticity properties at room temperature but rather the lack of water within the geopolymer during curing at low humidity. However, it is difficult to assert that PEG is responsible for the unusually high mechanical properties. These could also be explained by the presence of residual stresses following the rapid evacuation of water.

Storing samples at room temperature and low humidity after 28 days of storage at high humidity does not result in a significant increase in mechanical properties (Figure 6). The properties remain stable. The PEG band is almost not detected in infrared spectroscopy (Figure 8). In the case of a hypothesis where PEG acts as a mechanical binder, it is possible that it has been degraded by the basic environment at high humidity and can no longer play a binding role during the transition to low humidity. Alternatively, PEG may have been evacuated from the structure during the gradual formation of the geopolymer gel, or two days at low humidity might be insufficient for its solidification, particularly within the filament's core. Whatever remains inside the structure might not be present in a sufficient quantity to be detectable. Since the geopolymer network has already formed, and the PEG in liquid form at high humidity has been excluded from this network, it can no longer act as a binder at low humidity. In the scenario where high mechanical properties at low humidity result from residual stresses, it is not possible to achieve higher mechanical properties by lowering the humidity. The geopolymer network is already formed without being influenced by the rapid drainage of water. These residual constraints have no reason

to reappear. The non-detection of PEG may be due to degradation or its presence in too small a quantity.

4.2. Influence of Porosity and Shaping on Mechanical Properties

The results presented in Section 3.4 highlight the correlation between the compressive mechanical properties and sample porosity. Molded geopolymers exhibit a power law relationship between the two parameters, enabling the estimation of compressive strength based on envelope densities (Figure 14). However, this law proves less effective for the most porous lattices. This less good agreement for the samples obtained by direct ink writing could be explained by the inherent difficulty in achieving a flat surface for compression testing, leading to increased uncertainties in measurements. But it could also be due to the different fracture mechanisms of the molded foams, linked to the progressive fracture of the filaments and the presence of the millimeter scale of porosity. The study of the fracture surfaces and the tomography of the filaments containing PEG reveal the existence of cracks prior to any testing (Figure 17, cracks are highlighted by red circles), potentially influencing structural failure. The compression curves of architectural structures display numerous irregularities, likely attributed to the propagation of these pre-existing cracks and the gradual fracture of filaments.

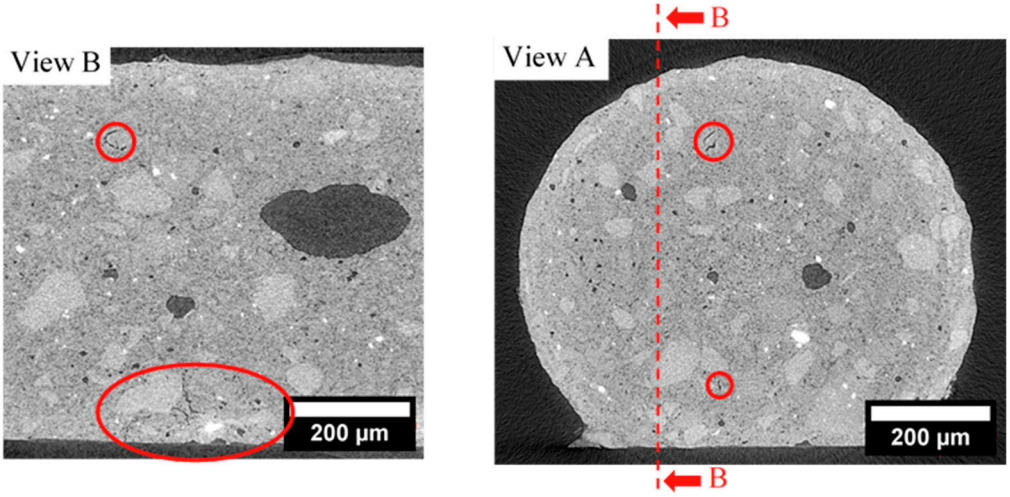

Figure 17. The microtomography of a filament of composition GP 0Al F having been stored for 3 days at 70 °C and 100% relative humidity. View B is the right view of the section placed on view A. The cracks are highlighted by red circles.

An exact comparison of these results with the literature proves challenging due to the dependence of these mechanical properties on various parameters, including raw materials, additives, curing conditions, and the type and morphology of blowing agents.

However, the average compressive strength of G 0Al M (50.8 MPa) closely aligns with that reported by Rowles and O'Connor (51.3 MPa) for geopolymers of similar composition, although the article does not specify the density of the samples [24].

Regarding molded foams, those produced in previous studies by incorporating aluminum powder typically exhibit envelope densities ranging from 0.4 to 0.8 g.cm^{-3} for a compressive strength between 0.4 and 3.7 MPa [25,26]. The foams generated in this work fall within this range and are therefore satisfactory.

For lattices, GP 0Al R has a compressive strength a little higher than that obtained by Franchin et al. [27] for geopolymer lattices of similar composition and porosity (11.5 MPa for 49.8% total porosity versus 18.3 MPA for 51.1% total porosity in this study). Gonçalves et al. [11] produced structures with a compressive strength of 17.3 ± 1.1 MPa for a total porosity of 65.9%. It is important to highlight that in those studies, porosity was induced by adjusting the spacing between filaments, whereas in our research, a significant part of the porosity is located inside the filament itself. A study closer to ours was carried out by

Oliveira et al. [12] who added porous fillers (activated carbon and hydrotalcite) into the geopolymer paste and printed structures with a compressive strength of 5.2 ± 0.8 MPa for a total porosity of 67.2 ± 0.2%.

5. Conclusions

This article studies the mechanical properties of metakaolin-based geopolymers shaped by molding and 3D printing.

It appears that the mechanical properties of extruded geopolymers in bending vary significantly depending on the humidity and temperature of the environment. Filaments containing PEG cured under low humidity conditions demonstrate unusually high mechanical properties (>115 MPa after 28 days) compared to filaments cured at high humidity (between 20 and 30 MPa after 28 days). These elevated mechanical properties are not stable and decrease when samples transition from dry to humid environments (<30 MPa).

Polyethylene glycol, added to enable the 3D printing of geopolymers, may be responsible for the abnormally high mechanical properties observed under low humidity. However, it is difficult to determine whether these observations are really due to a mechanical binder role played by PEG and/or to the presence of residual stresses. Additional studies are needed to clarify this point and to better understand the interactions of PEG with the geopolymer and the water available in the environment.

Under room temperature and low humidity curing conditions, the insufficient presence of water impedes complete geopolymerization, leading to mechanical properties that are both unstable and significantly low when exposed to high humidity (5 MPa). Conversely, storing samples at room temperature and high humidity results in consistently stable mechanical properties. Elevating the storage temperature accelerates geopolymerization, appearing to be rapid enough to offset water evacuation at low humidity and achieve complete geopolymerization. However, despite this, the samples cured at low humidity still display mechanical instability in response to humidity fluctuations.

Opting for printing and curing under high humidity conditions appears to be the most judicious decision for achieving samples with both complete geopolymerization and consistently stable mechanical properties. The strategic combination of high humidity with storage temperatures of 50 °C or 70 °C emerges as an effective approach to accelerate geopolymerization without compromising the mechanical integrity of the samples.

This work also focused on the influence of the shaping technique and porosity on the mechanical properties of geopolymers.

For molded geopolymers, a significant correlation emerged between compressive strength and envelope density. However, this correlation proves less pertinent for lattices, particularly those containing aluminum powder. The divergence suggests potential differences in fracture mechanisms between the two sample types. omplementary in situ monitoring of the compression test by X-ray tomography would be interesting to follow the initiation and propagation of cracks.

Author Contributions: Conceptualization, C.Z., E.P. and L.G.; methodology, C.Z., E.P. and L.G.; validation, C.Z., E.P. and L.G.; formal analysis, C.Z., E.P. and L.G.; investigation, C.Z.; resources, C.Z., E.P. and L.G.; data curation, C.Z.; writing—original draft preparation, C.Z.; writing—review and editing, C.Z., E.P., K.J. and L.G.; visualization, C.Z.; supervision, E.P., K.J. and L.G.; project administration, E.P.; funding acquisition, E.P., L.G. and K.J. All authors have read and agreed to the published version of the manuscript.

Funding: This work was supported by the LABEX iMUST of the University of Lyon (ANR-10-LABX-0064), created within the "Plan France 2030" set up by the French government and managed by the French National Research Agency (ANR). INSA Lyon through "Enjeu Energie" and IngéLyse (FR CNRS 3411) are acknowledged for their financial support.

Institutional Review Board Statement: Not applicable.

Informed Consent Statement: Not applicable.

Data Availability Statement: Data are contained within the article. Raw data can be made available upon request to the authors.

Acknowledgments: Special thanks to Sylvain MEILLE (MATEIS) for helpful discussion.

Conflicts of Interest: The authors declare no conflicts of interest. The funders had no role in the design of the study; in the collection, analyses, or interpretation of data; in the writing of the manuscript; or in the decision to publish the results.

References

1. Duxson, P.; Fernández-Jiménez, A.; Provis, J.L.; Lukey, G.C.; Palomo, A.; van Deventer, J.S.J. Geopolymer technology: The current state of the art. *J. Mater. Sci.* **2007**, *42*, 2917–2933. [CrossRef]
2. Rovnaník, P. Effect of curing temperature on the development of hard structure of metakaolin-based geopolymer. *Constr. Build. Mater.* **2010**, *24*, 1176–1183. [CrossRef]
3. Perera, D.S.; Uchida, O.; Vance, E.R.; Finnie, K.S. Influence of curing schedule on the integrity of geopolymers. *J. Mater. Sci.* **2007**, *42*, 3099–3106. [CrossRef]
4. Samuel, D.; Kriven, W.M. Depth dependence of hardness and reaction in metakaolin-based geopolymers cured at low humidity. *J. Am. Ceram. Soc.* **2024**, *107*, 543–560. [CrossRef]
5. Kirschner, A.V.; Harmuth, H. Investigation of geopolymers binders with respect to their application for building materials. *Ceramics-Silikáty* **2004**, *48*, 117–120.
6. Novais, R.M.; Ascensão, G.; Ferreira, N.; Seabra, M.P.; Labrincha, J.A. Influence of water and aluminium powder content on the properties of waste-containing geopolymer foams. *Ceram. Int.* **2018**, *44*, 6242–6249. [CrossRef]
7. Al-Noaimat, Y.A.; Ghaffar, S.H.; Chougan, M.; Al-Kheetan, M.J. A review of 3D printing low-carbon concrete with one-part geopolymer: Engineering, environmental and economic feasibility. *Case Stud. Constr. Mater.* **2023**, *18*, e01818. [CrossRef]
8. Archez, J.; Texier-Mandoki, N.; Bourbon, X.; Caron, J.F.; Rossignol, S. Adaptation of the geopolymer composite formulation binder to the shaping process. *Mater. Today Commun.* **2020**, *25*, 101501. [CrossRef]
9. Ma, S.; Fu, S.; Yang, H.; He, P.; Sun, Z.; Duan, X.; Jia, D.; Colombo, P.; Zhou, Y. Exploiting bifunctional 3D-Printed geopolymers for efficient cesium removal and immobilization: An approach for hazardous waste management. *J. Clean. Prod.* **2024**, *437*, 140599. [CrossRef]
10. Jin, H.; Zhang, Y.; Zhang, X.; Chang, M.; Li, C.; Lu, X.; Wang, Q. 3D printed geopolymer adsorption sieve for removal of methylene blue and adsorption mechanism. *Colloids Surfaces A Physicochem. Eng. Asp.* **2022**, *648*, 129235. [CrossRef]
11. Gonçalves, N.P.F.; Olhero, S.M.; Labrincha, J.A.; Novais, R.M. 3D-printed red mud/metakaolin-based geopolymers as water pollutant sorbents of methylene blue. *J. Clean. Prod.* **2023**, *383*, 135315. [CrossRef]
12. Oliveira, K.G.; Botti, R.; Kavun, V.; Gafiullina, A.; Franchin, G.; Repo, E.; Colombo, P. Geopolymer beads and 3D printed lattices containing activated carbon and hydrotalcite for anionic dye removal. *Catal. Today* **2022**, *390–391*, 57–68. [CrossRef]
13. Ma, S.; Liu, X.; Fu, S.; Zhao, S.; He, P.; Duan, X.; Yang, Z.; Jia, D.; Colombo, P.; Zhou, Y. Direct ink writing of porous SiC ceramics with geopolymer as binder. *J. Eur. Ceram. Soc.* **2022**, *42*, 6815–6826. [CrossRef]
14. Zoude, C.; Gremillard, L.; Prud'Homme, E. Combination of chemical foaming and direct ink writing for lightweight geopolymers. *Open Ceram.* **2023**, *16*, 100478. [CrossRef]
15. Yuan, J.; He, P.; Jia, D.; Yang, C.; Zhang, Y.; Yan, S.; Yang, Z.; Duan, X.; Wang, S.; Zhou, Y. Effect of curing temperature and SiO2/K2O molar ratio on the performance of metakaolin-based geopolymers. *Ceram. Int.* **2016**, *42*, 16184–16190. [CrossRef]
16. Prud'Homme, E.; Michaud, P.; Joussein, E.; Clacens, J.M.; Rossignol, S. Role of alkaline cations and water content on geomaterial foams: Monitoring during formation. *J. Non. Cryst. Solids* **2011**, *357*, 1270–1278. [CrossRef]
17. Pouhet, R. Formulation and Durability of Metakaolin-Based Geopolymers. Ph.D. Thesis, Université de Toulouse, Toulouse, France, 2015.
18. Khairuddin; Pramono, E.; Utomo, S.B.; Wulandari, V.; Zahrotul, A.W.; Clegg, F. FTIR studies on the effect of concentration of polyethylene glycol on polimerization of Shellac. *J. Phys. Conf. Ser.* **2016**, *776*, 012053. [CrossRef]
19. Prud'homme, E. Rôles du Cation Alcalin Et Des Renforts Minéraux Et Végétaux Sur Les Mécanismes de Formation de Géopolymères Poreux OU Denses. Ph.D. Thesis, Université de Limoges, Limoges, France, 2011.
20. Gibson, L.J.; Ashby, M.F. *Cellular Solids: Structure and Properties*, 2nd ed.; Cambridge University Press: Cambridge, UK, 1999.
21. Baird, J.A.; Olayo-Valles, R.; Rinaldi, C.; Taylor, L.S. Effect of molecular weight, temperature, and additives on the moisture sorption properties of polyethylene glycol. *J. Pharm. Sci.* **2010**, *99*, 154–168. [CrossRef] [PubMed]
22. Cyr, M.; Pouhet, R. Carbonation in the pore solution of metakaolin-based geopolymer. *Cem. Concr. Res.* **2016**, *88*, 227–235. [CrossRef]
23. Davidovits, J. *Geopolymer Chemistry and Applications*, 4th ed.; Institut Géopolymère: Saint-Quentin, France, 2015.
24. Rowles, M.; O'Connor, B. Chemical optimisation of the compressive strength of aluminosilicate geopolymers synthesised by sodium silicate activation of metakaolinite. *J. Mater. Chem.* **2003**, *13*, 1161–1165. [CrossRef]
25. Bai, C.; Colombo, P. Processing, properties and applications of highly porous geopolymers: A review. *Ceram. Int.* **2018**, *44*, 16103–16118. [CrossRef]

26. Kioupis, D.; Zisimopoulou, A.; Tsivilis, S.; Kakali, G. Development of porous geopolymers foamed by aluminum and zinc powders. *Ceram. Int.* **2021**, *47*, 26280–26292. [CrossRef]
27. Franchin, G.; Scanferla, P.; Zeffiro, L.; Elsayed, H.; Baliello, A.; Giacomello, G.; Pasetto, M.; Colombo, P. Direct ink writing of geopolymeric inks. *J. Eur. Ceram. Soc.* **2017**, *37*, 2481–2489. [CrossRef]